Polymer 50 (2009) 5837–5845

Contents lists available at ScienceDirect

Polymer

journal homepage: www.elsevier.com/locate/polymer

Surface morphology alignment of block copolymers induced by injection molding

Liang Fang, Ming Wei, Yingrui Shang, Lady Jimenez, David Kazmer, Carol Barry, Joey Mead*

NSF Nanoscale Science and Engineering Center for High-rate Nanomanufacturing, Department of Plastics Engineering, University of Massachusetts Lowell, One University Avenue, Lowell, MA 01854, USA

ARTICLE INFO

Article history:
Received 3 July 2009
Received in revised form
2 September 2009
Accepted 6 September 2009
Available online 30 September 2009

Keywords:
Block copolymer
Injection molding
Surface morphology orientation

ABSTRACT

Block copolymers are of increasing interest because of their nanometer-scale morphologies, which can be utilized in a range of applications, including nanolithography. Orientation of the domains can be controlled by part design and processing conditions in injection molding. In this work the surface morphology and alignment of block copolymers by mechanical flow fields from injection molding was investigated using a styrene–ethylene/butylene–styrene triblock copolymer (SEBS) and compared with the morphology induced by spin coating. Compared with the isotropic morphology found by spin coating and annealing, the surface domains were oriented in the flow direction. Increasing mold temperature and injection velocity enhanced the degree of orientation, whereas melt temperature had little effect. Smaller characteristic lengths were produced with higher mold temperatures and injection velocities.

1. Introduction

Block copolymers are of increasing interest because of their nanometer-scale morphologies [1], which can be utilized in a range of applications, including nanolithography [2–4]. Changes in composition ratio, molecular weight, and interaction parameter result in a range of nanometer structures of block copolymer, including spherical, cylindrical, gyroid, or lamellar morphologies. The self-assembly of block copolymers, however, tends to create domains with a high level of local order, but without long-range periodical alignment [5–8]. This behavior constrains the exploitation of block copolymers in the field of nanotechnology.

Understanding the phase morphology, particularly the surface morphology, developed under high-rate processes, such as extrusion and injection molding, will be required for the transition of block copolymer into practical applications. Mechanical flow fields from common polymer processing methods, including extrusion [9], injection molding [10], and compression molding [11,12], have been successfully applied to create long-range morphology alignment of bulk block copolymers. Rheometer studies have been applied to establish the relationship between the domain structure orientation and parameters of the mechanical flow field [13–15]. These studies have investigated the bulk morphology, but not the surface orientation.

Given that the potential applications using bulk morphology control and orientation are limited, but surface morphology control is important for potential applications in fabrication of functional devices [2–4,16]. Most investigations [16–23] have turned their attention to surface morphology control and orientation for block copolymer thin films, rather than thick structures produced in processes such as injection molding and extrusion. Electric fields [17,18], magnetic fields [19], and chemically nano-patterned substrates [20,21] have been utilized to manipulate the domain orientations of block copolymer thin films. Chaikin and coworkers [22,23] used mechanical flow fields (by pressing a polydimethylsiloxane pad onto a block copolymer thin film and then applying a horizontal force to induce the shear stress) to orient the surface morphology, resulting in oriented structures with millimeter length scales.

It is of considerable commercial importance to understand the surface morphology behavior of block copolymers under high rates typical of conventional plastics processing, where orientation directions can be controlled conveniently by proper part design, especially in injection molding. All of the prior studies on morphology orientation for block copolymers in high-rate processes (injection molding, extrusion) have investigated the bulk, not the surface. Studies of the surface orientation have been done only on thin films, primarily from solution, rather than the melt state. There is, however, limited information on the phase morphology of block copolymers at the surface using large scale processing equipment, where the flow fields are more complex and the material is in the melt state. Additionally, understanding of the orientation behavior in these processes facilitates tool design for more complex devices and orientations.

Therefore, the purpose of this paper is to study the surface morphology and alignment of block copolymers by mechanical

* Corresponding author. Tel.: +978 934 3446; fax: +978 934 4056.
E-mail address: joey_mead@uml.edu (J. Mead).

0032-3861/$ – see front matter © 2009 Elsevier Ltd. All rights reserved.
doi:10.1016/j.polymer.2009.09.013

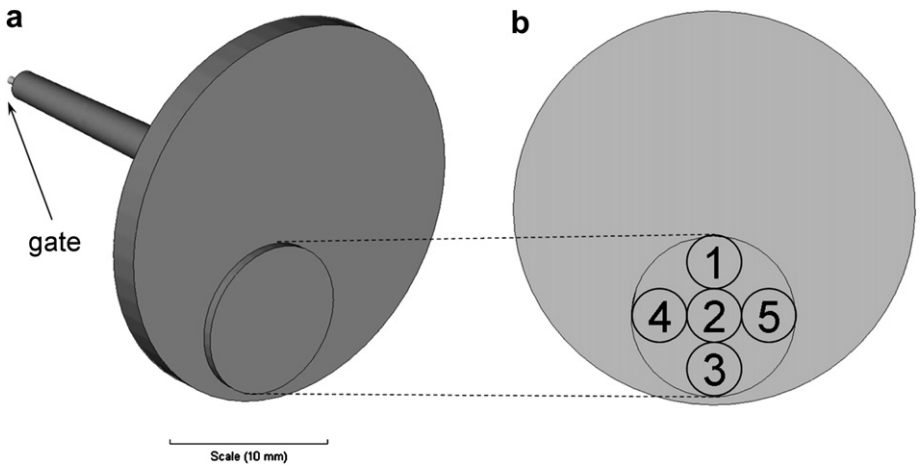

Fig. 1. Circular SEBS part processed by injection molding: (a) 3D schematic diagram of the part with the gate located in the center and (b) top view of the examined circular region which has been further divided into five areas: (1) gate end, (2) center, (3) part end, (4) left side, and (5) right side.

flow fields given by injection molding and to discuss the basic relationships between domain geometry and processing parameters. The effect of injection molding process parameters on the resultant surface morphology of a styrene–ethylene/butylene–styrene triblock copolymer (SEBS) was investigated in this work. Changes in mold temperature, T_{mold}; melt temperature, T_{melt}; and injection velocity, $V_{injection}$, were evaluated experimentally and simulated using commercial software. Phase domain alignment and characteristic length were analyzed by atomic force microscopy and Fast Fourier Transformation (FFT).

2. Experimental section

All work was performed using a commercial styrene–ethylene/butylene–styrene triblock copolymer (SEBS) block copolymer (Kraton, MD 6932). The material contained 20 wt% of polystyrene (PS) and had a melt index of 80 g/10 min (at 230 °C and 5 kg) [24].

2.1. Spin coating and annealing

To obtain the equilibrium surface morphology, the SEBS film was prepared by spin coating. The SEBS solution (20 wt% SEBS in toluene) was spin-coated at 300 rpm for 60 s on steel plates. After the material was dry, the sample was annealed for 168 h (seven days) at 110 °C before characterization.

2.2. Injection molding

Circular parts of SEBS were fabricated using a micro-injection molding machine (Nissei, model: AU3E). The SEBS was dried overnight prior to injection molding. As shown in Fig. 1a, the center-gated parts had a diameter of 25 mm and a nominal thickness of 2 mm. A 10 mm diameter insert located at one side of the part produced a round region that protruded 0.5 mm from the part surface. Experiments were originally performed using a steel mold (average roughness (Ra) of injection molding tool steel varies from 0.07 to 1.5 μm, based on the surface polishing [25]), however, the sample surfaces were found to be too rough for AFM analysis of the surface morphology. Vapor gold coated silicon wafers with a surface roughness of only 1.8 nm (determined by AFM topography images) were utilized as the insert. A 0.4 mm thick polytetrafluoroethylene sheet was installed behind the wafer to protect it from breaking at high melt pressures [26]. When examining the phase morphology over the 2.5 mm thick region, the surface was divided into five different regions (gate end, center, part end, left side and right side) as illustrated in Fig. 1b.

Six groups of SEBS specimens were injection molded using the processing conditions shown in Table 1. To evaluate the effects of processing temperatures, two melt temperatures, 204 and 240 °C, and two mold temperatures, 24 and 71 °C, were utilized. Three injection velocities representing 5%, one-third, and two-thirds of the machine capacity (i.e., 10, 50, and 100 mm/s) were investigated keeping the melt and mold temperatures constant. The hold and back pressures were 100 MPa and 15 MPa, respectively, whereas the cooling time was set at 30 s.

2.3. Simulation and characterization

Commercial software, MoldFlow Plastics Institute (MoldFlow Corp., version 6.2), was used to simulate the melt behavior, including shear rate, temperature, and viscosity, during injection molding. The SEBS material properties were not available in the material database for the simulation software, so a replacement (Dynaflex G7940, GLS Corp.) was selected. The surface morphologies of the SEBS specimens were examined by non-contact mode atomic force microscopy (AFM, PSIA XE-150). AFM image analysis software XEI (PSIA Corp., version 1.5) was utilized to conduct the Fast Fourier Transformation (FFT) analysis of corresponding AFM phase images. The FFT spectrum cannot merely determine if the morphology is isotropic or anisotropic, but can also be used to calculate the characteristic length of the block copolymer [27–29].

3. Results and discussion

3.1. Initial morphology of SEBS film by spin coating

In order to study the effect of mechanical field on the surface morphology of SEBS, thin films of SEBS were first prepared by spin coating and then annealing for seven days. The surface was

Table 1
Processing conditions used during injection molding.

Trial	Melt temperature (°C)	Mold temperature (°C)	Injection velocity (mm s^{-1})
A	204	24	2
B	240	24	2
C	240	71	2
D	240	24	10
E	240	24	50
F	240	24	100

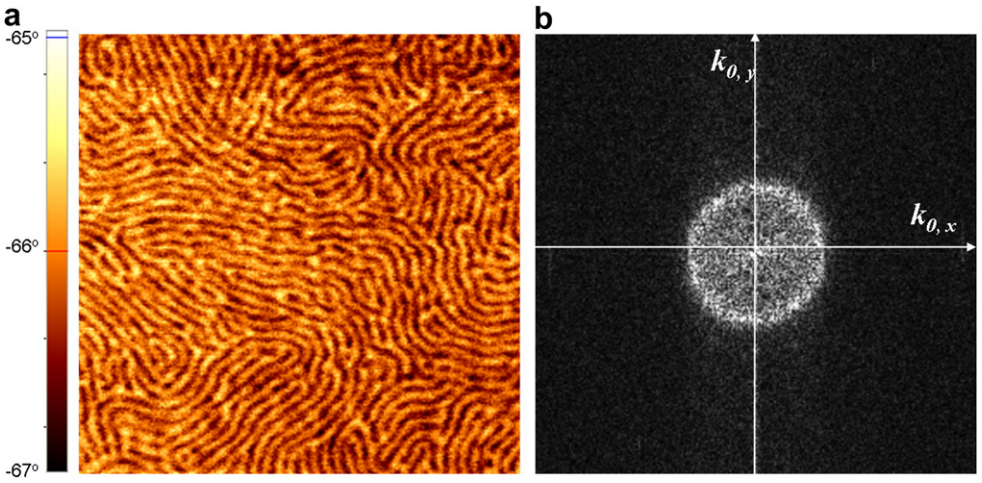

Fig. 2. SEBS film prepared by spin coating and then annealing for seven days: (a) AFM phase image with scan size of 1 μm × 1 μm and (b) corresponding Fast Fourier Transformation diagram.

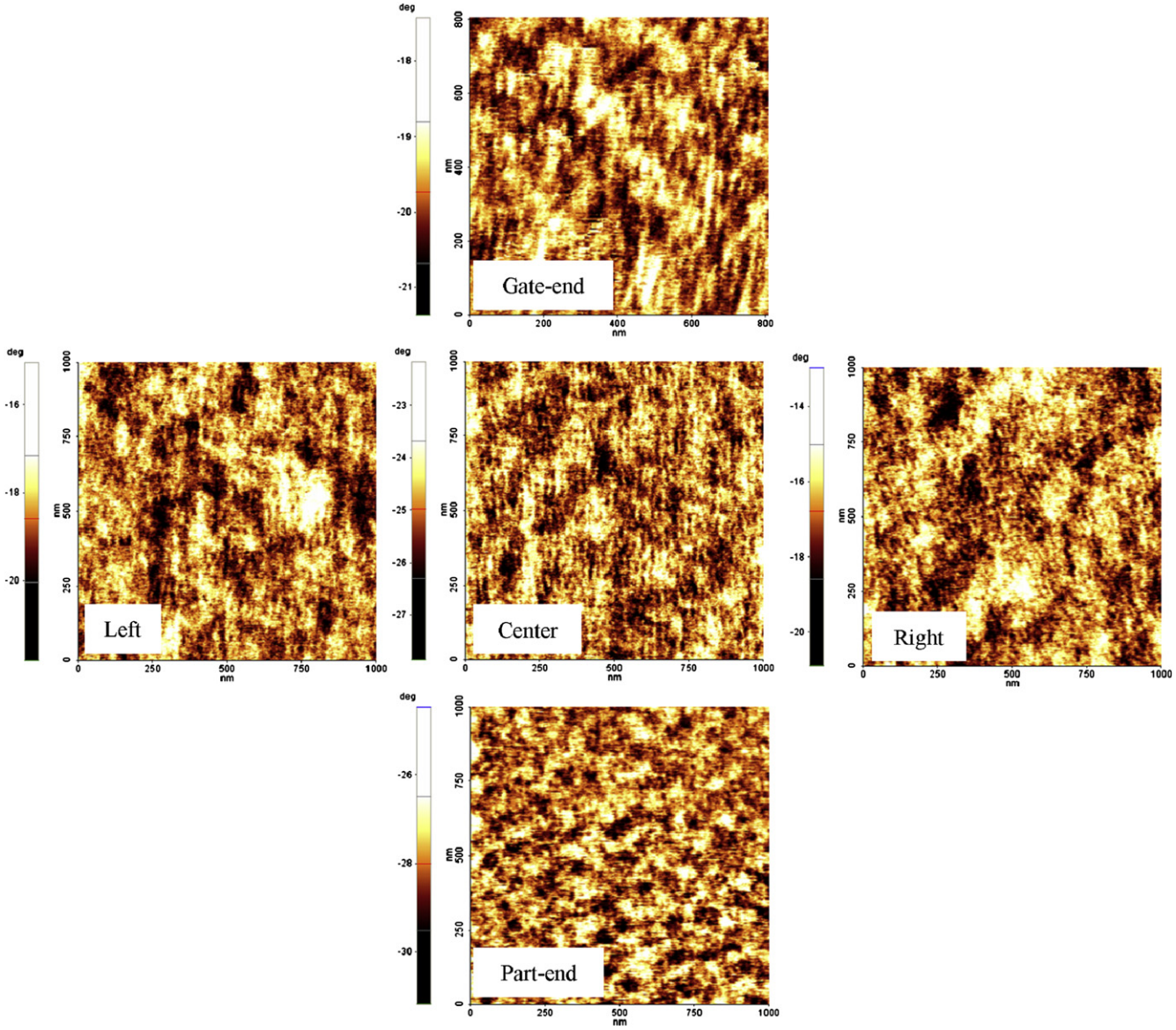

Fig. 3. AFM phase images of the five regions examined for SEBS specimens prepared by injection molding with $T_{melt} = 204$ °C and $T_{mold} = 24$ °C, which are presented according to the sequence shown in Fig. 1b. The scan size of the gate end region is 0.8 μm × 0.8 μm, while the others are 1 μm × 1 μm.

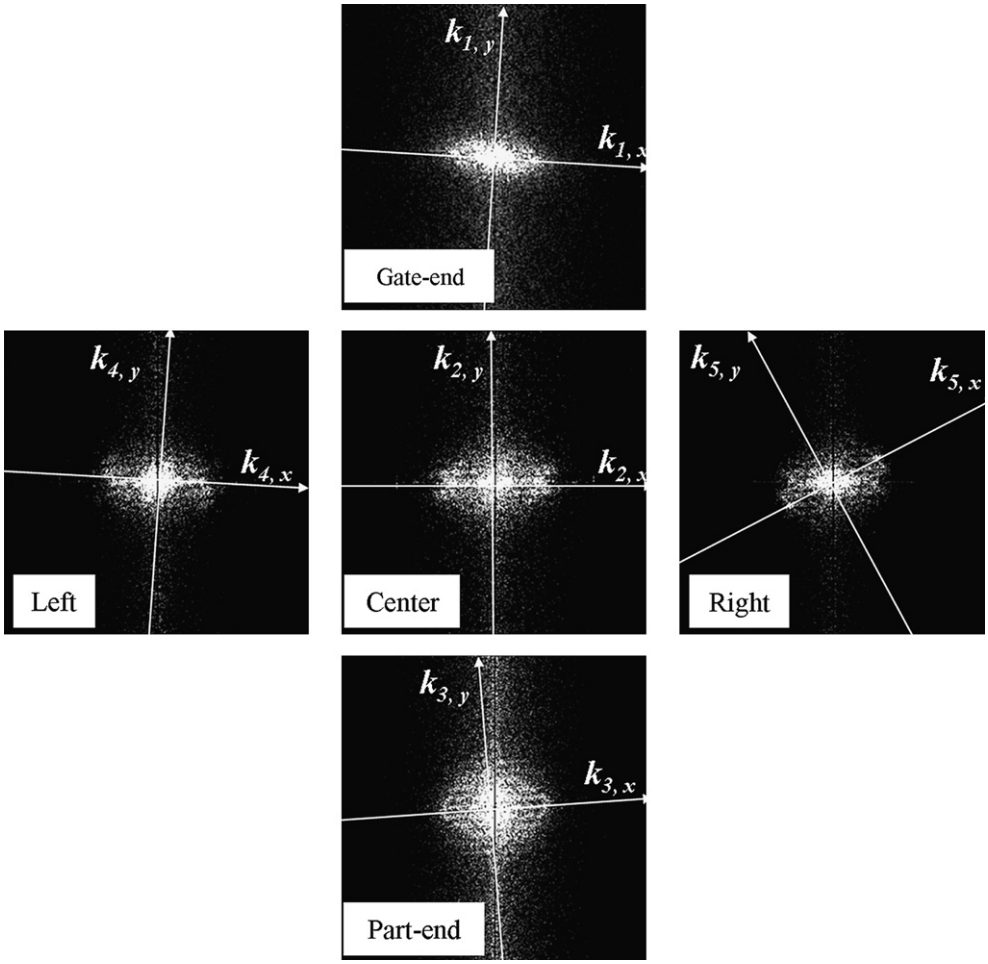

Fig. 4. Corresponding FFT diagrams in five examined regions as shown in Fig. 3. Numbers 1–5 represent the gate end, center, part end, left side, and right side, respectively.

assumed to have the equilibrium morphology of the SEBS thin film because the long-time annealing step allowed the incompatible components to phase separate completely. Fig. 2a shows the surface morphology of the SEBS film as revealed by the AFM phase images, where the two phase morphologies of the material can be clearly seen. In this system the polystyrene (PS) domains appear as the bright regions, as it is generally accepted that brighter regions in AFM phase images are attributed to the block copolymer component with higher modulus [30–33]. Fig. 2a also illustrates that the polystyrenes domains do not have any long-range order. The corresponding FFT diagram of the spin-coated morphology of SEBS is presented in Fig. 2b. The symmetric ring confirms that the wave patterns had a uniform average wavelength and the equilibrium morphology of the SEBS was isotropic. Therefore, the thermodynamically balanced characteristic length was 34.5 nm calculated by $1/k^*$ [27–29]. Here $k^* = k_{0,x}{}^* = k_{0,y}{}^*$, where k^* is the wave vector where the FFT amplitude of the round halo is a maximum.

3.2. Surface morphology orientation from injection molding

The ability of mechanical flow fields from injection molding to induce the long-range orientation of phase structures of SEBS was then investigated. The injection molded samples (molded with melt and mold temperatures of 204 and 24 °C, respectively, and an injection velocity of 2 mm/s) were first compared with the spin-coated parts. Fig. 3 presents the AFM phase images of the surface morphologies for the five examined regions of the injection molded

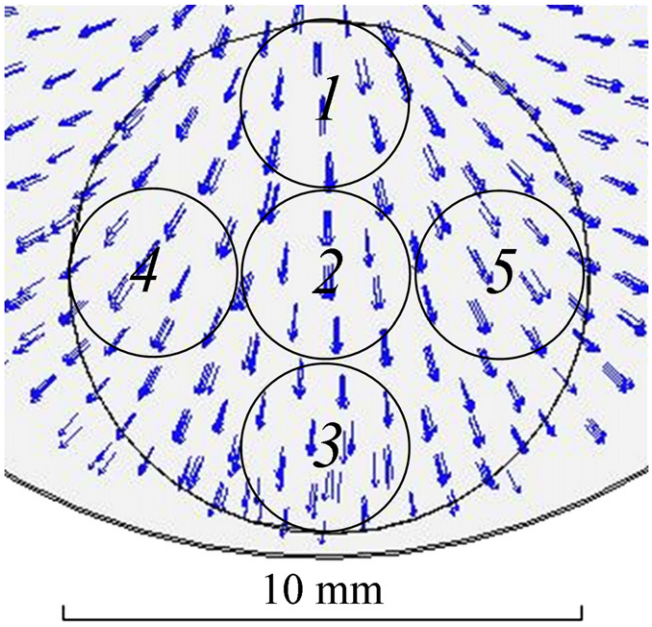

Fig. 5. Diagram of simulated melt velocity field while the melt filling the cavity. Blue arrows indicate the directions of melt flow with the five examined regions are shown by five small circles: (1) gate end, (2) center, (3) part end, (4) left side, and (5) right side. (For interpretation of the references to colour in this figure legend, the reader is referred to the web version of this article.)

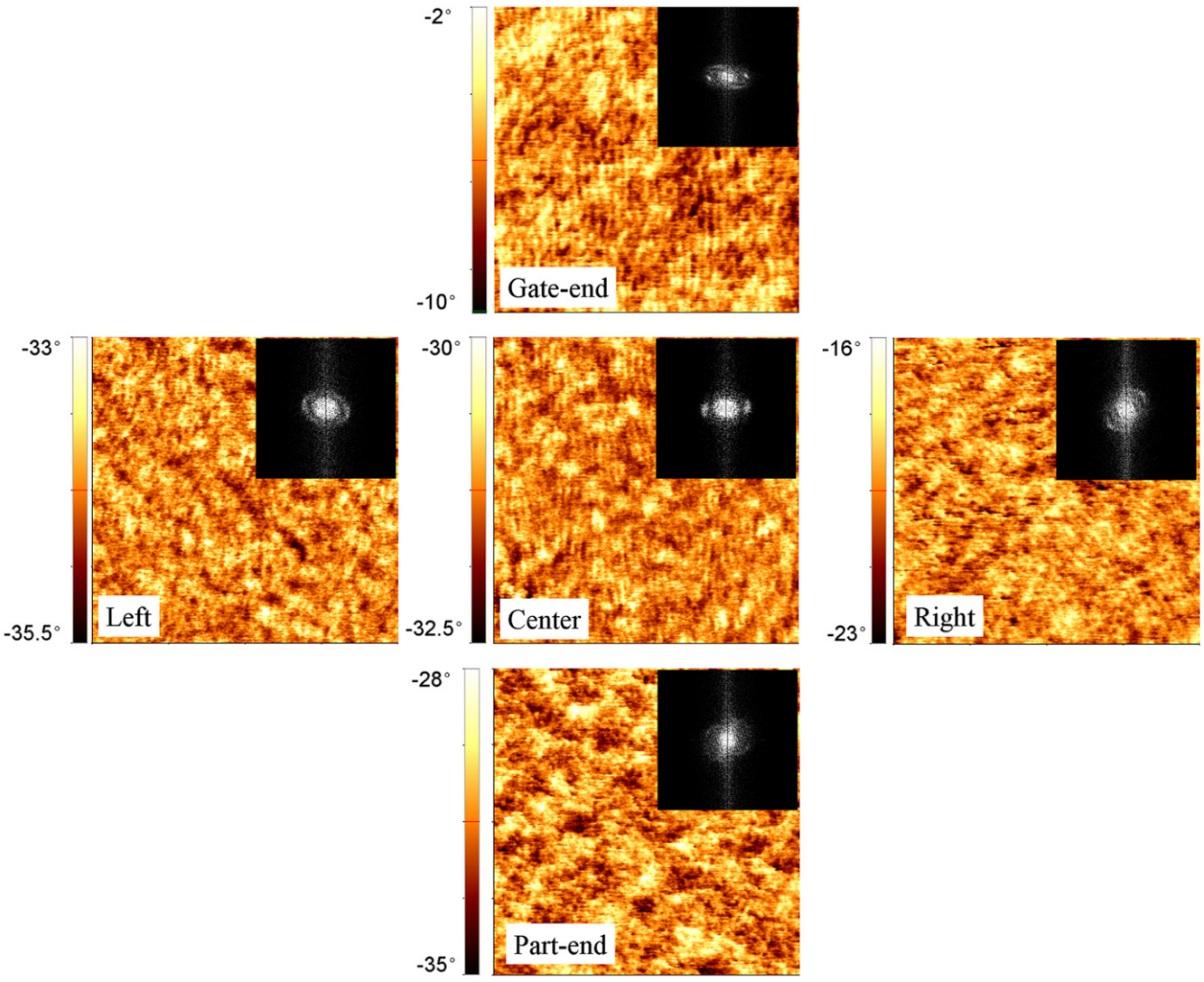

Fig. 6. AFM phase images and corresponding FFT diagrams of five regions examined of SEBS specimens prepared at higher T_{melt} of 240 °C. The scan size of all five regions was 1 μm × 1 μm.

SEBS. Compared with equilibrium annealed morphology, the characteristic length appeared smaller. More importantly, the polystyrene domains were oriented and the long-range alignment directions varied for each of the different regions. The orientation degree of the part end, however, was weaker than that of the gate end.

The morphology alignment was supported by the corresponding FFT diagrams (Fig. 4). With an isotropic morphology, the FFT diagram formed a round halo as mentioned above. For an anisotropic morphology, the wave vector magnitude in the direction parallel to the orientation direction (y-axis), $k^*_{i,y}$ (where $i = 1, 2, 3, 4$, and 5 indicate the five different locations), was shifted towards smaller $k_{i,y}$ and became smaller than $k^*_{i,x}$. The isotropic halo thus became anisotropic and elliptical in shape. In these situations, characteristic length was determined from $1/k^*_{i,x}$ because the critical wave vector representing the characteristic length could only be obtained along the x-axis, which was perpendicular to the alignment direction. In addition, $k_{i,y}$ had different directions for each of the regions, indicating that the morphology orientation directions varied in the five examined regions.

Fig. 5 presents the simulated melt velocity field for these conditions. The arrows represent the flow directions of the SEBS melt, but also the direction of mechanical flow field induced by injection molding. Comparing the orientation direction of the morphology in each region in Fig. 3 and the direction of $k_{i,y}$ in Fig. 4 with its corresponding mechanical flow field direction in Fig. 5, it can be easily seen that the polystyrene domains were oriented along the mechanical field directions. Fig. 5 shows only the direction of the flow fields, however, the intensity of the field will vary from the gate to the part end, being much lower in intensity (velocity and pressure) at the part end [34]. Therefore, the surface morphology alignment of the block copolymers can be attributed to the mechanical flow which can be conveniently controlled by proper design of the part and its melt delivery (gate and runner) system.

3.3. Influence of different processing conditions

The block copolymer morphology became oriented in the direction of the mechanical flow field, but the morphology may also be affected by the injection molding parameters. Research on the bulk morphology in block copolymers has shown that orientation can be increased by shear rate [13] or shear strain [14,15]. These studies were performed using laboratory scale equipment which may not adequately capture the behavior in high-rate processing

conditions. In addition, injection molding is more complicated because mold and runner system design, as well as the processing conditions, can affect the flow throughout the part. Injection molding is also a high-rate processing technique, so the block copolymer typically cannot attain the equilibrium morphology. The time prior to vitrification of the macromolecular chains is critical and this time will be affected by the melt temperature, mold temperature, and injection velocity.

3.3.1. *Effect of processing temperatures*

To evaluate the influence of melt temperature, this temperature was increased from 204 to 240 °C, while keeping the mold temperature constant. As shown in Fig. 6, the polystyrene domains were oriented in the direction of the mechanical flow field. Corresponding FFT patterns indicated similar results with those obtained at the lower melt temperature (shown in Fig. 4). The degree of alignment in the end of fill (part end region) was also weaker than in the gate end section. The role of mold temperature in the evolution of morphology was then examined by increasing the mold temperature to 71 °C, while keeping melt temperature at 240 °C. As illustrated in Fig. 7, the higher mold temperature had a significant influence on the orientation behavior. In all five regions, a higher degree of orientation was produced at higher mold temperature as compared with those at low (24 °C) mold temperature (shown in Figs. 3 and 6, respectively). This orientation improvement was further substantiated by the more anisotropic elliptical shape of the FFT diagrams.

Most researchers define degree of orientation based on the deviation of the axis of the cylindrical domains from the shear direction, typically indicated by an angle theta [23,35,36]. Due to the diverging flow shown in Fig. 5, we were unable to use this convention. When Endoh et al. [37] investigated the influence of shearing time on surface morphology orientation of a semidilute polystyrene/diethyl malonate solution, they observed that the difference between the critical wave vectors parallel and perpendicular to the flow direction increased with flow time. Extending this observation for this work, the degree of orientation on the SEBS surfaces was quantified by calculating the ratio of $k^*_{i,y}/k^*_{i,x}$, where $k^*_{i,y}$ is the critical wave vector parallel to the flow direction and $k^*_{i,x}$ is the critical wave vector perpendicular to the flow direction These ratios are shown in Table 2. When $k^*_{i,y}/k^*_{i,x}$ equals 1 (as illustrated in Fig. 2b), the morphology is isotropic. As the morphology becomes more oriented

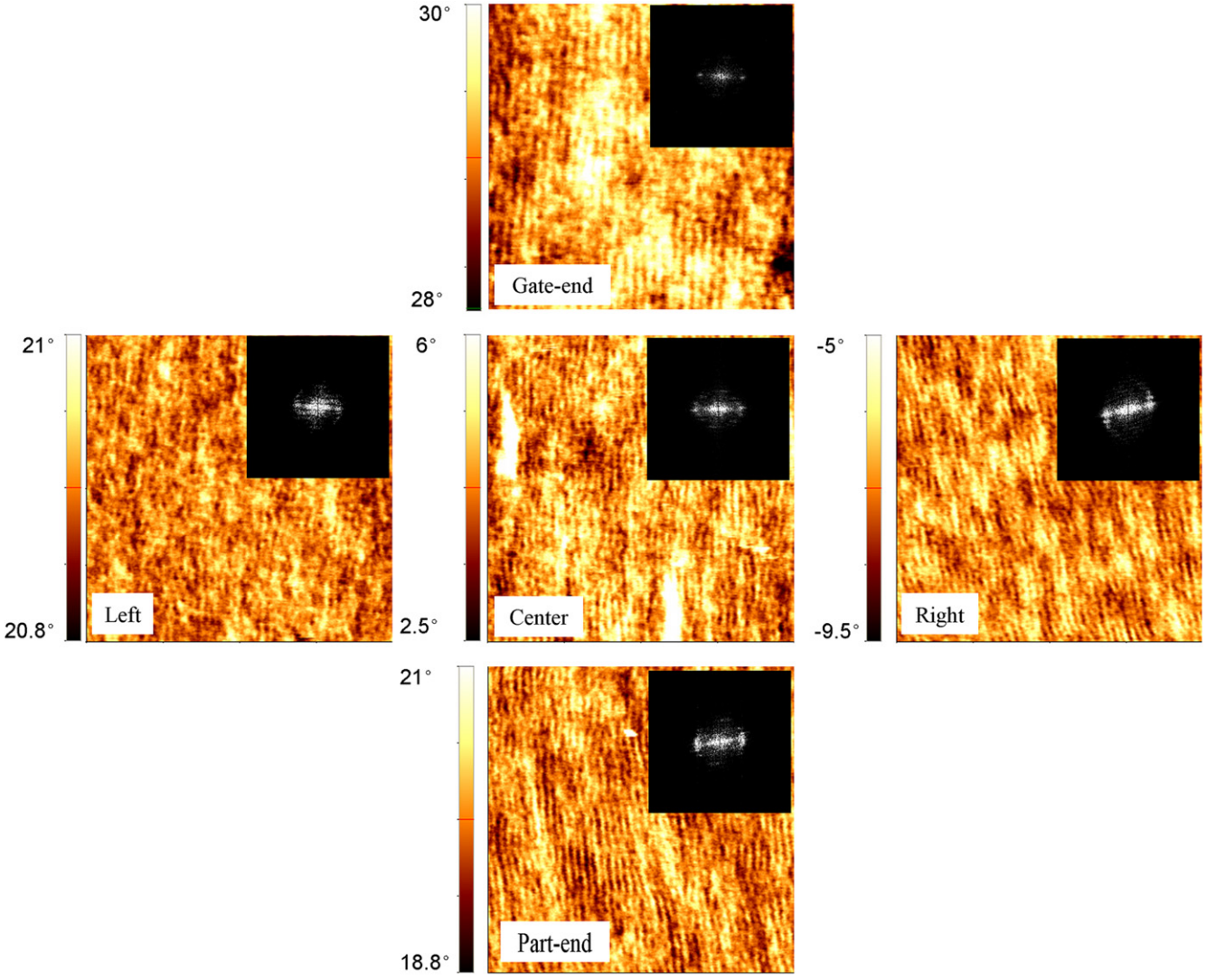

Fig. 7. AFM phase images and corresponding FFT diagrams of SEBS specimens prepared at higher $T_{mold} = 71$ °C. The scan size of the gate end region is 0.8 μm × 0.8 μm, whereas the others are 1 μm × 1 μm.

Table 2
Values of $k^*_{i,y}/k^*_{i,x}$ for each examined regions at different processing temperatures.

Locations	Trial 1	Trial 2	Trial 3
	$T_{melt} = 204\ ^\circ C$, $T_{mold} = 24\ ^\circ C$	$T_{melt} = 240\ ^\circ C$, $T_{mold} = 24\ ^\circ C$	$T_{melt} = 240\ ^\circ C$, $T_{mold} = 71\ ^\circ C$
Gate end	0.55	0.55	0.32
Left side	0.52	0.55	0.30
Center	0.52	0.54	0.31
Right side	0.55	0.54	0.32
Part end	0.80	0.94	0.32
Average	0.59 ± 0.12	0.62 ± 0.18	0.31 ± 0.01

in the y-axis direction, $k^*_{i,y}$, which represents the critical wave vector along the direction parallel to domain alignment, becomes smaller. In the case of perfect alignment, $k^*_{i,y}/k^*_{i,x}$ will be zero. As shown in Table 2, when the mold temperature was 24 °C, $k^*_{i,y}/k^*_{i,x}$ remained nearly constant for the gate end, center, left side, and right side locations, but was larger at the end of fill (part end). This finding indicates that the domains at the end of fill were less oriented. With an increase in mold temperature, however, the domain alignment behavior changed. First, the overall degree of domain alignment was greater for the higher mold temperature. Second, the higher mold temperature produced similar domain alignment in all five locations. In contrast, for a low mold temperature, an increase in melt temperature had little effect on the domain alignment, with the exception of the part end. The average ratio was 0.52–0.55 in all locations except the end of fill, where the values increased to 0.80–0.94.

The amount of orientation at the surface is the result of the amount of orientation induced by fountain flow (from shear flows down the cavity and elongational flows at the melt front) minus the amount of orientation that is removed by relaxation. This phenomenon is a complex dynamic between the viscosity of the melt and the solidification rate at the surface. The orientation of fibers or fillers [38–40], crystallites of semi-crystalline polymers [41,42], dispersed liquid crystalline polymer phase [43,44], and dispersed polymer domains in polymer blends [45,46] during injection molding has been attributed to fountain flow. When the hot melt reaches the cold mold, the oriented domains solidify quickly and the alignment is thus retained in the frozen/solid layer. Massé et al. [47] simulated the heat transfer of a polymer melt (235 °C melt temperature) contacting a mold at 60 °C; the polymer surface temperature was found to decrease to approximately 85 °C in the first 0.45 s. Since the processing temperatures used in this study are similar to those employed by Massé et al., the oriented domains on the surface were assumed to solidify rapidly when reaching the mold surface. As a result, relaxation of the oriented domains on the polymer surface was negligible and the degree of orientation on the surface was primarily controlled by the amount of orientation induced by fountain flow.

Fig. 8 presents simulations of the bulk temperature of the melt. As expected, the temperature of the melt is low at the walls and higher in the center. Comparing the two melt temperatures, the higher melt temperature produced a hotter core temperature, but the melt temperatures at the mold walls were similar with both melt temperatures (Fig. 8a,b). When the mold temperature was increased to 71 °C, the wall temperatures were higher, but still below the glass transition temperature of the hard phase, freezing in the induced orientation as shown in Fig. 8c. The core temperatures with this higher mold temperature were significantly higher. Li et al. [45] found that increasing the temperature of the melt increased the orientation of polycarbonate (PC) domains in a polyethylene (PE)/PC blend. Pantani and coworkers [48] observed that increasing mold temperature increased the surface orientation in isotactic polypropylene, even though the thickness of frozen layer was reduced. The simulation results and prior work suggest that the higher melt temperature at the flow front, allows for greater induced orientation of the SEBS domains, which is then frozen when the material reaches the mold wall.

3.3.2. *Effect of injection velocity*

Injection velocity also impacted the resultant surface morphologies of SEBS specimens. Fig. 9 shows the surface morphology of injection molded SEBS as a function of injection velocity when melt temperature and mold temperature were held constant. Given that the part geometry and gate system remained the same, only the left regions of the part were studied.

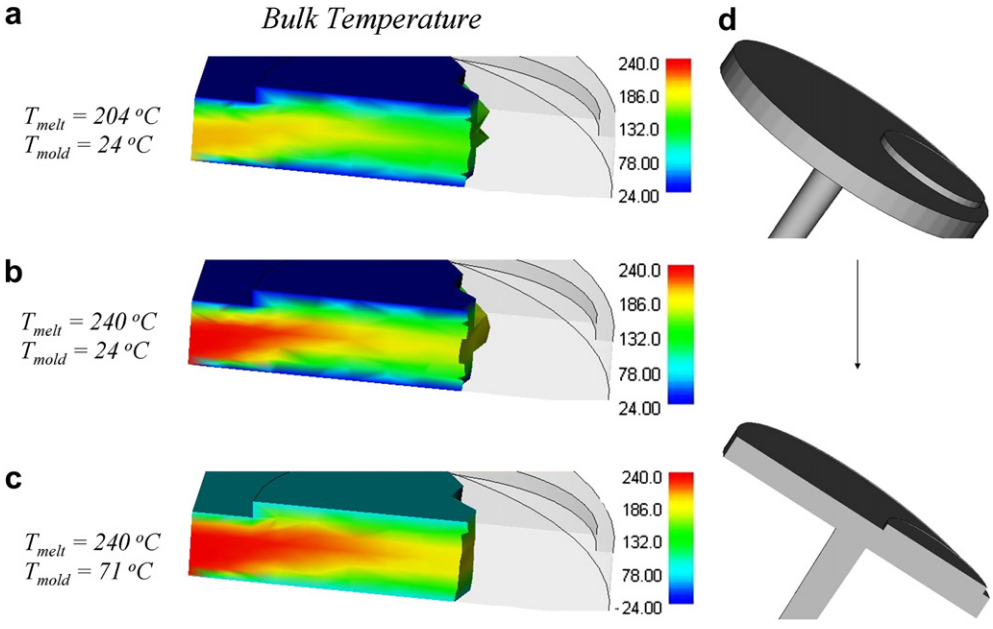

Fig. 8. Simulated temperatures during injection molding of SEBS parts at different processing temperatures. The processing temperatures varied in the three cases: (a) T_{melt} and T_{mold} were 204 and 24 °C, (b) T_{melt} and T_{mold} were 240 and 24 °C, and (c) T_{melt} and T_{mold} were 240 and 71 °C. Fig. 8d indicated the schematic diagram of the simulated area in the modeling.

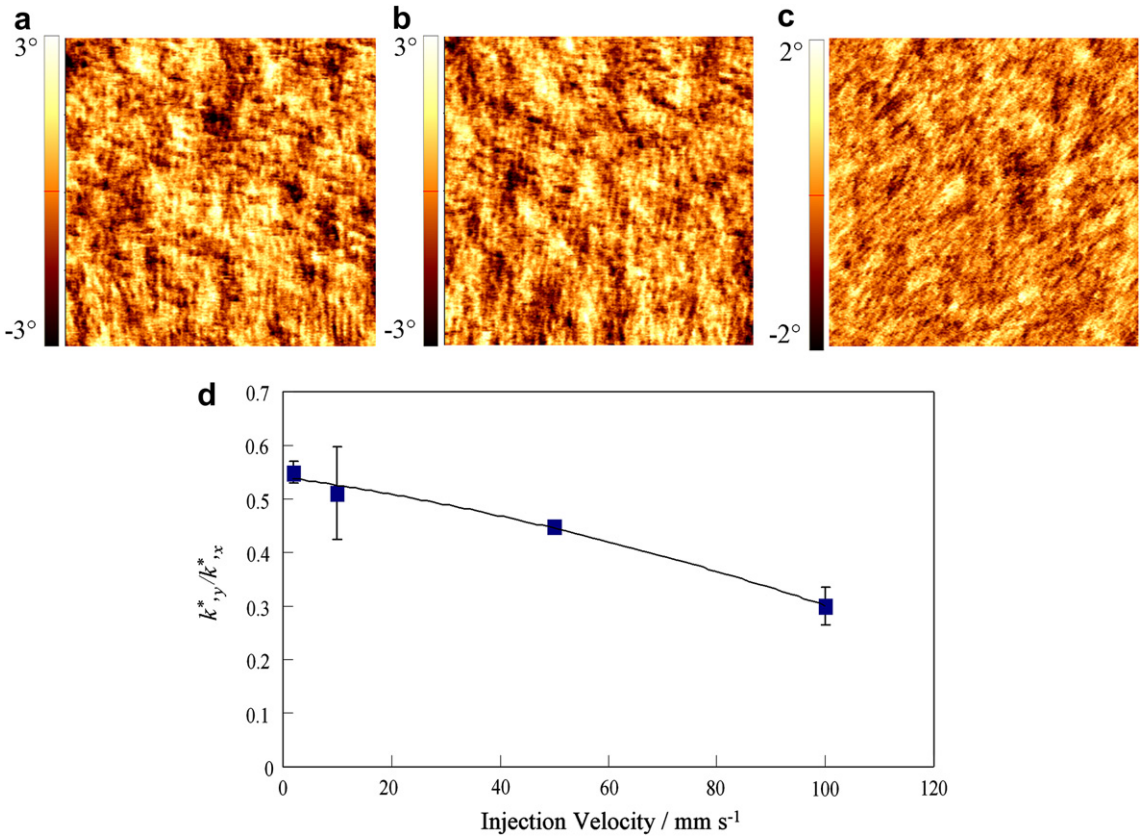

Fig. 9. AFM phase images of left regions of SEBS specimens fabricated by injection molding with injection velocities of (a) 10 mm/s, (b) 50 mm/s, and (c) 100 mm/s. The scan size is 1 μm × 1 μm. (d) The relationship between $k^*_{i,y}/k^*_{i,x}$ and injection velocity.

The orientation of the polystyrene domains increased with increasing injection velocity. Fig. 9d shows the $k^*_{i,y}/k^*_{i,x}$ values from the FFT. When the injection velocity was raised from 2 mm/s to 100 mm/s, the $k^*_{i,y}/k^*_{i,x}$ values reduced from 0.55 to 0.30, quantitatively showing the polystyrene domain alignment increased with increasing injection velocity. Similar results were also found by Pantani et al. [48] for the effect of injection velocity on the orientation of isotactic polypropylene in the skin layer. Higher orientation of carbon nanotubes (CNT) was obtained in the skin layer of a PC/CNT blend with increased injection velocity as reported by Villmow et al. [38].

Simulation results for the effect of injection velocity on the mechanical flow fields are shown in Fig. 10a–i. Both the shear rate and the temperature at the melt front were seen to increase with

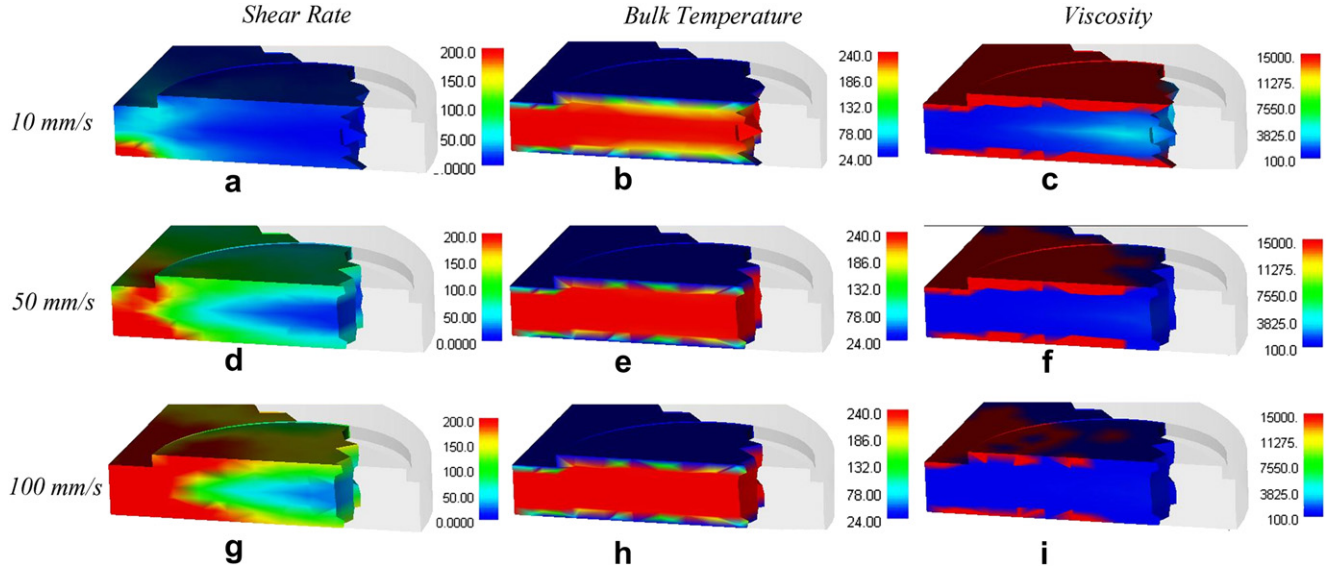

Fig. 10. Simulated parameters during injection molding of SEBS parts under three injection velocities, including (a, d, g) shear rate/s, (b, e, h) temperature/°C, and (c, f, i) viscosity/Pa-s $V_{injection}$ was respectively (a–c) 10 mm/s, (d–f) 50 mm/s and (g–i) 100 mm/s.

Table 3
Average values of characteristic length under different processing conditions. For trial A–C, the value is on the average of the five examined regions. For trial D–F, the values were only the average of the left regions.

Trial number	Processing conditions	Characteristic length/nm
A	$T_{melt} = 204\ ^\circ C$, $T_{mold} = 24\ ^\circ C$	30.1 ± 2.5
B	$T_{melt} = 240\ ^\circ C$, $T_{mold} = 24\ ^\circ C$	29.7 ± 5.0
C	$T_{melt} = 240\ ^\circ C$, $T_{mold} = 71\ ^\circ C$	25.5 ± 0.9
D	$V_{injection} = 10$ mm/s	29.4 ± 1.6
E	$V_{injection} = 50$ mm/s	26.7 ± 0.7
F	$V_{injection} = 100$ mm/s	23.8 ± 1.4

injection velocity (Fig. 10a–f) for a given processing temperature, especially the shear rate. Morrison et al. [13] have reported that increasing shear rates increased the orientation of polystyrene domains in an SBS block copolymer. Fig. 10g–i shows the viscosity distribution during SEBS melt filling. Viscosity of the melt is decreased with injection velocity from shear thinning. The combined effect of lower viscosity, higher shear rates and higher temperatures with increased injection velocity all act to increase the orientation of the polystyrene domains in the block copolymer.

3.3.3. Characteristic length of domains under different processing conditions

Injection molding is a high-rate polymer processing method. The time allowed for block copolymer to phase separate during injection molding is insufficient for the morphology to reach equilibrium. FFT can be used to obtain the characteristic length of the phase morphology of blends or block copolymers [27–29]. This characteristic length is related to the periodicity of the domains and thus domain size. Table 3 shows the effects of processing conditions on the evolution of the characteristic length. Compared with the equilibrium characteristic length calculated from the spin-coated specimen (34.5 nm) high-rate injection molding reduced the characteristic length. Samples compared immediately after molding and after 10 days exhibited no differences in characteristic length, therefore the results for the 10 days specimens are reported. Increasing mold temperature and injection velocity was found to slightly reduce the characteristic length further. This behavior is the result of orientation, which stretches the polystyrene cylindrical domains giving smaller measured values for the characteristic length, which is measured perpendicular to the long axis of the oriented domains. With increasing melt temperature the orientation was little varied, characteristic length thus remained nearly constant.

4. Conclusions

In this work, the injection molding parameters (mold temperature, melt temperature, and injection velocity) were investigated for their effects on the surface morphology of a styrenic block copolymer. Orientation of the domains was induced by injection molding and was found to vary from the gate to the part end. When the filling was slow, orientation increased with mold temperature, but not with melt temperature. Increased injection velocity was found to increase the domain orientation. Smaller characteristic lengths were produced with higher mold temperatures and injection velocities, as a result of greater orientation and domain elongation.

Acknowledgement

The authors would like to thank the support of the National Science Foundation (Award # NSF-0425826). The authors wish to thank Kraton, Inc. for the SEBS material and Nissei America for the injection molding machine.

References

[1] Hamley IW. The physics of block copolymers. Oxford: Oxford University Press; 1998.
[2] Segalman RA. Mater Sci Eng R 2005;48:191–226.
[3] Park C, Yoon JS, Thomas EL. Polymer 2003;44:6725.
[4] Darling SB. Prog Polym Sci 2007;32:1152.
[5] Bondzic S, Polushkin E, Schouten AJ, Ikkala O, Brinke GT. Polymer 2007;48:4723–32.
[6] van Dijk MA, van den Berg R. Macromolecules 1995;28:6773–8.
[7] Mclean RS, Sauer BB. Macromolecules 1997;30:8314–7.
[8] Magonov SN, Cleveland J, Elings V, Denley D, Whangbo MH. Surf Sci 1997;389:201–11.
[9] Keller A, Pedemonte E, Willmouth FM. Nature 1970;225:538.
[10] Huy TA, Adhikari R, Lüpke TH, Michler GH, Knoll K. Polym Eng Sci 2004;44:1534–42.
[11] Drzal PL, Barnes JD, Kofinas P. Polymer 2001;42:5633–42.
[12] Quiram DJ, Register RA, Marchand GR, Adamson DH. Macromolecules 1998;31:4891–8.
[13] Morrison FA, Mays JW, Muthukumar M, Nakatani AI, Han CC. Macromolecules 1993;26:5271–3.
[14] Morrison FA, Winter HH. Macromolecules 1989;22:3533–40.
[15] Morrison FA, Winter HH, Gronski W, Barnes JD. Macromolecules 1990;23:4200–5.
[16] Sakurai S. Polymer 2008;49:2781.
[17] Thurn-Albrecht T, Schotter J, Kästle GA, EMley N, Shibauchi T, Krusin-Elbaum L, et al. Science 2000;290:2126–9.
[18] Morkved TL, Lu M, Urbas AM, Ehrichs EE, Jaeger HM, Mansky P, et al. Science 1996;273:931–3.
[19] Osuji C, Ferreira PJ, Mao G, Ober CK, Van der Sande JB, Thomas EL. Macromolecules 2004;37:9903–8.
[20] Kim SO, Solak HH, Stoykovich MP, Ferrier NJ, de Pablo JJ, Nealey PF. Nature 2003;424:411–4.
[21] Yang XM, Peters RD, Nealey PF, Solak HH, Cerrina F. Macromolecules 2000;33:9575–82.
[22] Angelescu DE, Waller JH, Adamson DH, Deshpande P, Chou SY, Register RA, et al. Adv Mater 2004;16:1736–40.
[23] Pelletier V, Adamson DH, Register RA, Chaikin PM. Appl Phys Lett 2007;90:163105.
[24] Huan Y, Dave H, Jeff S. SPE Technol Papers 2006;64:1766–70.
[25] Griffiths CA, Dimov SS, Broussear EB, Hoyle RT. J Mater Process Technol 2007;189:418.
[26] Yoon SH, Lee JS, Park K, Mead JL, Matsui S, Barry CMF. Proceedings of SPIE – the International Society of Optical Engineeing 2006. Smart Medical and Biomedical Sensor Technology IV:6380.
[27] Kim YH, Okamoto M, Kotaka T. Macromolecules 2000;33:8113–6.
[28] Kim YH, Okamoto M, Kotaka T, Ougizawa T, Tchiba T, Inoue T. Polymer 2000;41:4747–9.
[29] Raczkowska J, Cyganic P, Budkowski A, Bernasik A, Rysz J, Raptis I, et al. Macromolecules 2005;38:8486–93.
[30] Wang Y, Song R, Li YS, Shen JS. Surf Sci 2003;530:136–48.
[31] Magonov SN, Elings V, Papkov VS. Polymer 1997;38:297–307.
[32] Motomatsu M, Mizutani W, Tokumoto H. Polymer 1997;38:1779–85.
[33] Garcia R, Tamayo J, Calleja M, Garcia F. Appl Phys A 1998;66:S309–12.
[34] Gerd P, Michaeli W. Injection molding: an introduction. New York: Hanser-Gardner Publications; 1995.
[35] BöKer A, Schmidt K, Knoll A, Zettl H, Hänsel H, Urban V, et al. Polymer 2006;47:849.
[36] Ruijter C, Mendes E, Boerstoel H, Picken SJ. Polymer 2006;47:8517.
[37] Endoh MK, Takenaka M, Hashimoto T. Polymer 2006;47:7271–81.
[38] Villmow T, Pegel S, Potschke P, Wagenknecht U. Compos Sci Technol 2008;68:777–89.
[39] Jeng MC, Fung CP, Li TC. Wear 2002;252:934–45.
[40] Vincent M, Giroud T, Clarke A, Eberhardt C. Polymer 2005;46:6719–25.
[41] Kim KH, Isayev AI, Kwon K, van Sweden C. Polymer 2005;46:4183–203.
[42] Zhu PW, Edward G. Polymer 2004;45:2603–13.
[43] Rendon S, Burghardt WR, Bubeck RA, Thomas LS, Hart B. Polymer 2005;46:10202–13.
[44] Tan LP, Joshi SC, Yue CY, Lam YC, Hu X, Tam KC. Acta Mater 2003;51:6269–76.
[45] Li ZM, Qian ZQ, Yang MB, Yang W, Xie BH, Huang R. Polymer 2005;46:10466–77.
[46] Porfyrakis K, Assender HE, Robinson IM. Polymer 2002;43:4769–81.
[47] Massé H, Arquis É, Delaunay D, Quilliet Le, Bot PH. Int J Heat Mass Transfer 2004;47:2015–27.
[48] Pantani R, Coccorullo I, Speranza V, Titomanlio G. Prog Polym Sci 2005;30:1185–222.